RESEARCH ARTICLE

Key Points:
- Q10 and microbial decomposition model can both capture 4 year observations
- Long-term trajectories of soil C dynamics differ among Q10 and microbial models
- We urge caution in interpreting future soil C dynamics from current models

Uncertainty in the fate of soil organic carbon: A comparison of three conceptually different decomposition models at a larch plantation

Yujie He[1], Jinyan Yang[2,3], Qianlai Zhuang[1,4], Anthony D. McGuire[5], Qing Zhu[1], Yaling Liu[1], and Robert O. Teskey[2]

[1]Department of Earth, Atmospheric, and Planetary Sciences, Purdue University, West Lafayette, Indiana, USA, [2]Warnell School of Forestry and Natural Resources, University of Georgia, Athens, Georgia, USA, [3]Center for Ecological Research, Northeast Forestry University, Harbin, China, [4]Department of Agronomy, Purdue University, West Lafayette, Indiana, USA, [5]U.S. Geological Survey, Alaska Cooperative Fish and Wildlife Research Unit, University of Alaska Fairbanks, Fairbanks, Alaska, USA

Abstract Conventional Q10 soil organic matter decomposition models and more complex microbial models are available for making projections of future soil carbon dynamics. However, it is unclear (1) how well the conceptually different approaches can simulate observed decomposition and (2) to what extent the trajectories of long-term simulations differ when using the different approaches. In this study, we compared three structurally different soil carbon (C) decomposition models (one Q10 and two microbial models of different complexity), each with a one- and two-horizon version. The models were calibrated and validated using 4 years of measurements of heterotrophic soil CO_2 efflux from trenched plots in a Dahurian larch (*Larix gmelinii* Rupr.) plantation. All models reproduced the observed heterotrophic component of soil CO_2 efflux, but the trajectories of soil carbon dynamics differed substantially in 100 year simulations with and without warming and increased litterfall input, with microbial models that produced better agreement with observed changes in soil organic C in long-term warming experiments. Our results also suggest that both constant and varying carbon use efficiency are plausible when modeling future decomposition dynamics and that the use of a short-term (e.g., a few years) period of measurement is insufficient to adequately constrain model parameters that represent long-term responses of microbial thermal adaption. These results highlight the need to reframe the representation of decomposition models and to constrain parameters with long-term observations and multiple data streams. We urge caution in interpreting future soil carbon responses derived from existing decomposition models because both conceptual and parameter uncertainties are substantial.

1. Introduction

Soils are the largest carbon (C) repository in the terrestrial biosphere, releasing 60–75 Pg C to the atmosphere each year through decomposition [*Schimel*, 1995; *Schlesinger and Andrews*, 2000]. Previous studies suggested that decomposition rates may respond more positively to increasing temperature than photosynthetic rates [*Ise et al.*, 2010; *Mahecha et al.*, 2010; *Smith and Dukes*, 2013], potentially initiating a positive feedback between the biosphere and warming of the climate system. Thus, projected soil organic C (SOC) dynamics and microbial activity under future climate change are central to understanding ecosystem responses to climate change and their feedbacks to climate.

Current "state-of-the-art" process-based biogeochemical models are built on the basis of current consensus within the scientific community on how to represent key ecosystem processes. In modeling decomposition, the response of decomposition to temperature has traditionally been characterized with a first-order Q10 relationship that originated from empirical observations in the 19th century [*van't Hoff*, 1898] and later evolved into various forms of Q10 or Arrhenius functions [*Lloyd and Taylor*, 1994; *Sierra*, 2012]. Such formulations are commonly used in contemporary biogeochemical models [*Friedlingstein et al.*, 2006; *Todd-Brown et al.*, 2013]. However, significant uncertainty exists due to (1) conceptual uncertainty associated with fundamental physiological processes that determine responses of soil carbon dynamics [*Wieder et al.*, 2013] and (2) parameter uncertainty within the same conceptual approach [*Todd-Brown et al.*, 2013]. In addition, recent studies that reveal some discrepancies between model outputs and experimental data [*Allison et al.*, 2010; *Wieder et al.*, 2013] argue for a paradigm shift in representing that soil C dynamics as traditional model structure
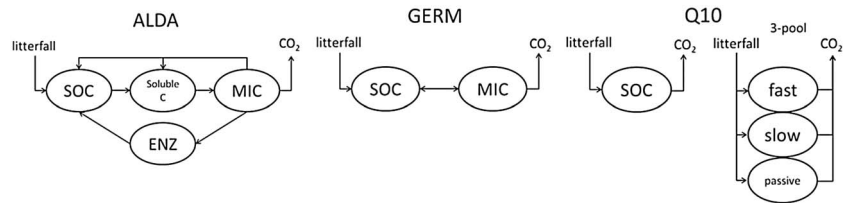
Figure 1. Schematic diagram of the three models.

may omit key mechanisms [*Davidson et al.*, 2012; *Wieder et al.*, 2013], such as the ephemeral augmentation of soil respiration under warming [*Luo et al.*, 2001; *Melillo et al.*, 2002; *Oechel et al.*, 2000] and the direct microbial control over soil C dynamics [*Allison et al.*, 2010; *Lawrence et al.*, 2009; *Wieder et al.*, 2013].

In spite of recent advances in modeling soil C dynamics and model comparison efforts [*Li et al.*, 2014; *Tuomi et al.*, 2008], it is unclear whether conceptually different schemes can reproduce observed decomposition (heterotrophic respiration, R_H) from field studies. It is also not clear how the long-term trajectories of soil C dynamics differ among traditional Q10 and microbial decomposition models. To answer these two questions, we evaluated three conceptually different decomposition model structures, including one Q10 model and two microbial models with different complexities, using the observed R_H fluxes from trenched plots over a 4 year period in deciduous forest. The two microbial models had different mechanistic complexities: a relatively simple two-pool model with a microbial biomass pool (MIC) and a SOC pool, and a more complex four-pool microbial model which included an additional extracellular enzyme pool (ENZ) and soluble C pool. Each structure was tested using one-horizon and two-horizon versions, where the two-horizon architecture was implemented to account for differences in decomposability between the O and the A horizons. For comparison, we used a one-horizon version of Q10 model which had one uniform SOC pool, as well as a Q10 model that had three compartments (three-pool Q10 model): a highly labile fast turnover C pool, a resistant slow turnover C pool, and a passive C pool [*Coleman and Jenkinson*, 1996; *Parton et al.*, 1993; *Schädel et al.*, 2014]. We first calibrated all seven decomposition models using an inverse estimation technique. We then used the calibrated models to simulate soil C decomposition dynamics. We hypothesized that (1) all models would capture the variation in observed soil R_H for the measurement period at model parameterization and validation stage; and (2) conventional Q10 models would not reproduce realistic long-term SOC dynamics under warming scenarios.

2. Methods

2.1. Model Description

The Q10 model follows the formulation described in *Fan et al.* [2008] and *Wickland and Neff* [2008]:

$$k(\theta, T) = k^* \times \left[\theta_c^2 - (\theta - \theta_c)^2 \right] \times Q_{10}^{(T-15^\circ C)/10} \tag{1}$$

$$dSOC/dt = -k \times SOC \tag{2}$$

where θ is the volumetric soil moisture, T is soil temperature (°C), θ_c is the optimum volumetric moisture content corresponding to maximum decomposition rate, and k^* is the optimum inherent decomposition rate at $\theta = \theta_c$ and $T = 15$°C. In the three-pool Q10 model, k^* varies among all three compartments. The simpler microbial model, which is based on *German et al.* [2012] (hereafter referred to as GERM), is a two-pool model with microbial biomass pool (MIC) and a SOC pool. The more complex four-pool microbial model is a hybrid version based on *Allison et al.*'s [2010] microbial-enzyme model and *Davidson et al.*'s [2012] DAMM model (hereafter referred to as ALDA) (Figure 1). A detailed description of this model can be found in *He et al.* [2014]. The two microbial models share a similar structure where SOC dynamics is directly regulated by either MIC or ENZ via a Michaelis-Menten enzyme kinetic function and the maximum reaction rate (Vmax, h^{-1}) follows Arrhenius temperature function:

$$DECAY = V\max 0_{SOC} \times \exp\left(-\frac{Ea_{SOC}}{R \times (T + 273)} \right) \times Enz\,(or\,MIC) \times \frac{SOC}{kM_{SOC} + SOC} \tag{3}$$

where Ea_{SOC} is the activation energy for SOC decay (J mol^{-1}), R is the ideal gas constant (8.314 J mol^{-1} K^{-1}), and T is soil temperature (°C) under which reaction occurs. kM_{SOC} (mg SOC cm^{-3} soil) is the corresponding Michaelis-Menten half-saturation constant.

HE ET AL.

2

To investigate whether representing depth-resolved processes influences the simulation of future SOC dynamics [*Knorr et al.*, 2005; *Yi et al.*, 2010], we constructed a two-horizon and a one-horizon version for each decomposition model. The two-horizon model explicitly simulates soil C dynamics in different soil horizons (i.e., O horizon, which contains discernable particulate organic matter, and A horizon, which occurs just below the O horizon). The thickness of each horizon is reassigned to different soil layers each year based on total simulated thickness of that horizon [*He et al.*, 2014], thus allowing the vertical temperature and moisture profiles to correspond with changing the thickness of the soil column. By distinguishing soil horizons we were also able to partition SOC into components with different intrinsic turnover rates, i.e., the more labile (O) versus the more recalcitrant (A) SOC. The one-horizon model combines the SOC in the O and A horizons into a single horizon and thus a single SOC pool. The three-pool Q10 model is also one horizon, but partitions total SOC stock into three compartments with different intrinsic decomposability.

2.2. Inverse Estimation of Model Parameters
2.2.1. Site Description and Observational Constraints

Soil CO_2 efflux and physical environmental data were collected at a site at the Maoershan Ecosystem Research Station in China (127°30–34′E, 45°20–25′N) dominated by Dahurian larch (*Larix gmelinii* Rupr.), a typical forest ecosystem in that region. A detailed description of site characteristics can be found in *Wang et al.* [2006]. This site has three replicate fixed plots (20 m × 30 m) with four R_H sampling subplots (50 cm × 50 cm) which were trenched to be free of live vegetation. In each R_H subplot, one polyvinyl chloride collar (10.2 cm inside diameter × 6 cm height) was installed [*Wang and Yang*, 2007]. To minimize artifacts associated with trenching disturbance [*Bond-Lamberty et al.*, 2011; *Jassal and Black*, 2006; *Lavigne et al.*, 2004], we only used measured R_H data that were collected two or more months after trenching. Soil surface CO_2 fluxes from trenched plots were measured with a Li-Cor 6400 portable CO_2 infrared gas analyzer connected with a Li-6400-09 chamber (Li-Cor Inc., Lincoln, NE, USA) biweekly from 2004 to 2007. Biweekly data were averaged to monthly resolution for consistency. Soil temperature and gravimetric water content were measured at 2 cm and 10 cm depths near each collar concurrently with R_H measurements. Soil temperature was measured with a digital long-stem thermometer. Soil water content was determined by taking soil samples at two depths and dried at 70°C to a constant mass. To account for the potential that estimated microbial respiration included decomposition of preexisting roots [*Drake et al.*, 2012; *Graham et al.*, 2012], we calculated the CO_2 efflux caused by the decomposition of labile components from dead root detritus based on root biomass [*Wang et al.*, 2006], the generalized models of fine root decay rate with respect to latitude [*Silver and Miya*, 2001] and the published decay rate for coarse roots [*Landsberg and Gower*, 1997], as was done in *Wang and Yang* [2007]. Calculated root decay was then subtracted from measured soil CO_2 efflux. Note that the soil at this site contains only a minimal amount of clay. Measured thickness, bulk density, SOC content, and microbial biomass of each soil horizon were collected as initial states and fixed parameters for the models (Table 1) [*Liu and Wang*, 2010; *Yang and Wang*, 2005]. The light and heavy fraction of the organic matter of the O and A horizons was determined by density fractionation [*Zhao*, 2013]. Light fraction is regarded as highly labile, whereas heavier amorphous material (heavy fraction) is regarded as more recalcitrant [*Boone*, 1994; *Tan et al.*, 2007; *Trumbore*, 1993]. The measured light and heavy fraction of the soil was used as prior for the inverse modeling of three-pool Q10 model parameters (Table 1).

2.2.2. Assimilation Scheme and Model Validation

Under Bayesian framework, the posterior probability density function (PDF) p_{post} of a sample from the joint parameter distribution $\boldsymbol{\theta}$ is a function of the prior probability of joint parameter p_{prior} and observation $\mathbf{x}$:

$$p_{post}(\boldsymbol{\theta}|\mathbf{x}) = \frac{L(\mathbf{x}|\boldsymbol{\theta})\, p_{prior}(\boldsymbol{\theta})}{\int L(\mathbf{x}|\boldsymbol{\theta}) p_{prior}(\boldsymbol{\theta}) d\boldsymbol{\theta}} \tag{4}$$

The denominator on the right-hand side is the marginal distribution of $\mathbf{x}$; therefore, given a realization of observation, the denominator is a constant and then can be ignored in the optimization. We assume that the prior distribution is uniform, and all observations are independently and identically distributed and follow a normal distribution, the likelihood $L(\boldsymbol{\theta}|\mathbf{x})$ can be formed as

$$L(\mathbf{x}|\boldsymbol{\theta}) = \prod_{i=1}^{n} \frac{1}{\sqrt{2\pi\sigma_i^2}} \exp\left[-\frac{1}{2}\frac{(f(\boldsymbol{\theta},t_i)-x_i)^2}{\sigma_i^2}\right] \tag{5}$$

where n is the number of observations $x_1, x_2, \ldots, x_n$ at time $t_1, t_2, \ldots, t_n$. σ_i is the standard deviation of each observation due to observation noise and measurement error, thus σ_i can differ among individual

Table 1. Soil Physical Metrics and MIC/SOC Ratio of Different Horizon (O and A Horizons) Types of the Needleleaf Deciduous Forest Stand in This Study

Metrics		O	A	References
Bulk density (g cm^{-3})	Mean	0.87	1.1	[*Yang and Wang*, 2005]
	STD (*n*)	0.45 (9)	0.05 (9)	
Organic carbon fraction (%)	Mean	5.1	4.1	[*Yang and Wang*, 2005]
	STD (*n*)	1.2 (9)	0.93 (9)	
Porosity (%)	Mean	64.8	59.2	[*Fan et al.*, 2004]
	STD (*n*)	-	-	
Particle density (g cm^{-3})	Mean	2.47	2.75	-
	STD (*n*)	-	-	
Horizon thickness (cm)	Mean	4.11	14.22	[*Yang and Wang*, 2005]
	STD (*n*)	1.6 (9)	8.47 (9)	
MIC/SOC (%)	Summer Mean	0.054	0.045	[*Liu and Wang*, 2010]
	STD (*n*)	0.002 (3)	0.001 (3)	
	Winter Mean	0.09	0.1	
	STD (*n*)	0.003 (3)	0.002 (3)	
Fraction of light-fraction SOM[a]	Mean	0.14	0.04	[*Zhao*, 2013]
	STD (*n*)	0.09 (10)	0.01 (10)	
Fraction of heavy-fraction SOM	Mean	0.8	0.87	[*Zhao*, 2013]
	STD (*n*)	0.09 (10)	0.05 (10)	

[a]SOM = Soil organic matter.

observations. However, because we lack the information necessary to determine how σ_i varies with each measurement, we made a simplification to assume constant σ_i for all observations. Applying a "log transformation" to the likelihood and ignoring the constant terms, we obtained the following cost functions to assimilate measured trenched plot soil efflux with the seven models (three structures × two versions + one 3-pool Q10):

ALDA:

$$
\text{Obj} = W_{\text{resp}} \times \sum_{i=1}^{k} \left(\text{Resp}_{\text{obs},i} - \text{Resp}_{\text{sim},i} \right)^2 + W_{\text{mic/soc}} \times \sum_{i=1}^{l} \left(\frac{\text{MIC}_{\text{sim},i1}}{\text{SOC}_{\text{sim},i1}} - 0.001 \right)^2
$$
$$
+ W_{\text{mic/soc}} \times \sum_{i=1}^{l} \left(\frac{\text{MIC}_{\text{sim},i2}}{\text{SOC}_{\text{sim},i2}} - 0.0005 \right)^2 + W_{\text{cue}} \times \sum_{i=1}^{k} \left(\text{CUE}_{\text{sim},i} - 0.5 \right)^2 \qquad (6)
$$

GERM:

$$
\text{Obj} = W_{\text{resp}} \times \sum_{i=1}^{k} \left(\text{Resp}_{\text{obs},i} - \text{Resp}_{\text{sim},i} \right)^2 + W_{\text{mic/soc}} \times \sum_{i=1}^{l} \left(\frac{\text{MIC}_{\text{sim},i1}}{\text{SOC}_{\text{sim},i1}} - 0.001 \right)^2
$$
$$
+ W_{\text{mic/soc}} \times \sum_{i=1}^{l} \left(\frac{\text{MIC}_{\text{sim},i2}}{\text{SOC}_{\text{sim},i2}} - 0.0005 \right)^2 \qquad (7)
$$

Q10:

$$
\text{Obj} = W_{\text{resp}} \times \sum_{i=1}^{k} \left(\text{Resp}_{\text{obs},i} - \text{Resp}_{\text{sim},i} \right)^2 \qquad (8)
$$

where the differences between the simulated decomposition (Resp$_{\text{sim}}$), the simulated ratio between microbial biomass and SOC ($\frac{\text{MIC}_{\text{sim}}}{\text{SOC}_{\text{sim}}}$), and the simulated carbon use efficiency (CUE$_{\text{sim}}$) and observations were minimized. The measured annual average $\frac{\text{MIC}}{\text{SOC}}$ of O (0.001) and A (0.0005) horizons are adopted from [*Liu and Wang*, 2010] (for the one-horizon model, the average $\frac{\text{MIC}}{\text{SOC}}$ was used). Simulated CUE was assumed to fluctuate around 0.5 as commonly reported in other studies [*Frey et al.*, 2013; *Manzoni et al.*, 2012; *Sinsabaugh et al.*, 2013]. $W_{\text{resp}}, W_{\text{mic/soc}}$, and W_{cue} are the weighting function set to 6.0×10^6, 1000, and 100, respectively, to reconcile the different magnitudes of metrics. The parameter *k* is the number of data pairs available to compare observation and simulation. See the supporting information for more details of the prior and optimized parameter values.

We applied a global optimization method known as the (shuffled complex evolution) [*Duan et al.*, 1992, 1994], which is an effective and efficient method specifically designed to obtain global convergence in

the presence of multiple regions of attraction under high-parameter dimensionality. We performed 100 independent optimization runs, each using different random number seed to determine the successive evolution steps. The resulting stationary distribution from the 100 runs converges to the joint parameter posterior PDF. The two-horizon ALDA model has the highest number of parameters of 16, and the simplest one-horizon Q10 model has only three parameters. It took on average ~200,000 and ~15,000 model evaluations to converge on the optimum parameter sets for the two models, respectively.

Because of limited data availability for calibration, we calibrated each model with the first 3 years of field-based decomposition estimates and validated each model with field-based decomposition estimates from the fourth year. The goodness-of-fit statistics between field-based and model simulation estimates of decomposition were calculated using all 4 years of estimates. Because trenched plot does not have litter inputs, the modeling system will equilibrate when decomposition reaches zero (microbial biomass equals zero); therefore, we did not start simulation from equilibrium but rather did a 1 year spin-up to stabilize the pool sizes. The initial prior ranges for model parameters were obtained from literature (e.g., *Allison et al.* [2010], *Knorr et al.* [2005], and *German et al.* [2012]), and were later expanded or shifted during the optimization process to ensure that posterior distribution was not truncated by the prior range (Tables S1–S3 in the supporting information).

2.3. Future Extrapolation

To examine how structural differences can affect projection, we conducted two sets of simulations: (1) control simulations with no litterfall input or warming (i.e., the natural projection of the initial SOC of a trenched plot that is expected to decrease over time) and (2) simulations with progressively increasing litter inputs and temperature. Monthly litterfall from an adjacent control plot was collected during 2005 using mesh-gridded cloth with diameter 1 m (J. Yang, unpublished data, 2005; Figure S1 in the supporting information). Our total annual litterfall C amounts to about $180 \, g \, C \, m^{-2} \, yr^{-1}$ and is comparable to data published in other studies [e.g., *Zhang et al.*, 2008]. We simulated an increase in litterfall input by 3% every 10 years for future projection (Figure S1b in the supporting information). The 3% litterfall increase rate (34% increase over 100 years) is chosen as a moderate scenario based on a suite of seven global vegetation models that simulated 34–70% increase in net primary production (NPP) under the HadGEM2-ES Representative Concentration Pathway 8.5 (RCP 8.5) climate and CO_2 scenario [*Friend et al.*, 2014]. We also assumed that a constant fraction of NPP is allocated to litterfall. Litterfall was added to multihorizon and three-pool Q10 models according to an exponentially decreasing curve [*Fan et al.*, 2008] (70% to the O horizon and 30% to the A horizon for multihorizon model; 50%, 30%, and 20% for the fast, slow, and passive pools of three-pool Q10 model, respectively).The surface temperature was increased progressively using the Representative Concentration Pathway 8.5 (RCP 8.5) from 2000 to 2100 with a projected overall change by 4.9°C (approximately 0.05°C yr^{-1} global average) [*Arora et al.*, 2011, 2013]. The scenario we used was a generalized scenario and was not specific to the region of the field study. Soil moisture values for the warming simulation were based on measurements from the control plot to avoid bias because soil water content in trenched plots is often higher than that of vegetated plot due to lack of transpiration [*Hanson et al.*, 2000]. For the simplicity of the analysis, the projected change in soil moisture in this region was not considered due to its uncertainty under projected warming [*Seth et al.*, 2013].

3. Results and Discussion

3.1. Inverse Estimates of Parameters

The model evaluation statistics showed that all three models can reproduce the field-based estimate of R_H of the trenched plot reasonably well, with an adjusted R^2 ranging from 0.5 to 0.78 for two-horizon models and from 0.58 to 0.80 for one-horizon models (Table 2). The root-mean-squared error (RMSE) of all ensemble runs was highest for the two-horizon ALDA model ($0.0023 \, mg \, C \, cm^{-2} \, h^{-1}$) and lowest for the one-horizon GERM model ($0.0014 \, mg \, C \, cm^{-2} \, h^{-1}$). These results support our first hypothesis. The seasonal dynamics of the modeled soil CO_2 flux showed that all seven models could describe the monthly variations in the field-based efflux (Figure 2). The two-horizon GERM and ALDA models showed the most divergence among ensemble runs (larger error bar, Figures 2a and 2b), indicating that some of the parameters in these models were poorly constrained. Note that the near-zero winter R_H (November–March) exhibited in the field-based estimates is best captured by the ALDA model (Figures 2a and 2d).

Whether or not an individual parameter is well constrained can be revealed by its posterior PDF (Figure 3 and Table 3 for parameter descriptions). The posterior PDF of parameters representing SOC intrinsic

Table 2. Model Evaluation Statistics From Ensemble Inverse Parameter Estimation for Three Soil Models at a Needleleaf Deciduous Forest Site[a]
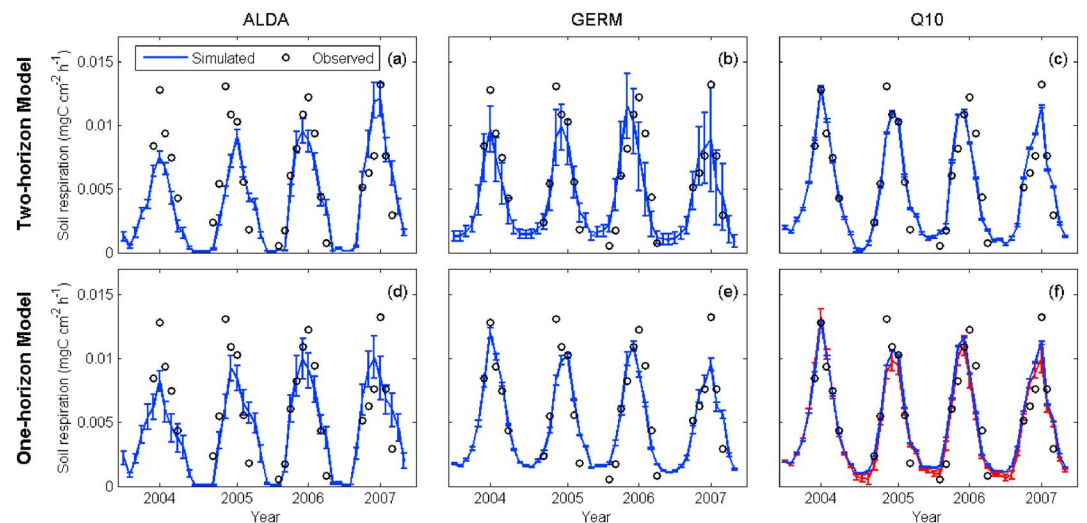
Model	RMSE (SD) $(mg\,C\,cm^{-2}\,h^{-1})$	Adjusted R^2 (SD)	Slope (SD)	Intercept (SD) $(mg\,C\,cm^{-2}\,h^{-1})$
	Two-horizon model			
ALDA	0.0023 (0.0003)	0.50 (0.07)	0.84 (0.1)**	0.0031 (0.0003)
GERM	0.0016 (0.0001)	0.68 (0.02)	0.92 (0.09)**	0.0015 (0.0011)
Q10	0.0015 (0.00001)	0.78 (0.003)	1.03 (0.02)**	−0.0002 (0.0001)
	One-horizon model			
ALDA	0.0019 (0.0001)	0.58 (0.05)	0.92 (0.1)**	0.0017 (0.0007)
GERM	0.0014 (0.0001)	0.78 (0.01)	1. 15 (0.04)**	−0.0008 (0.0002)
Q10	0.0015 (4.3e−8)	0.79 (0.001)	1.03 (0.0002)**	−0.0003 (1.9e−6)
Q10 (3-pool)	0.0017 (2.3e−5)	0.80 (0.005)	1.02 (0.046)**	−0.0001 (0.0003)

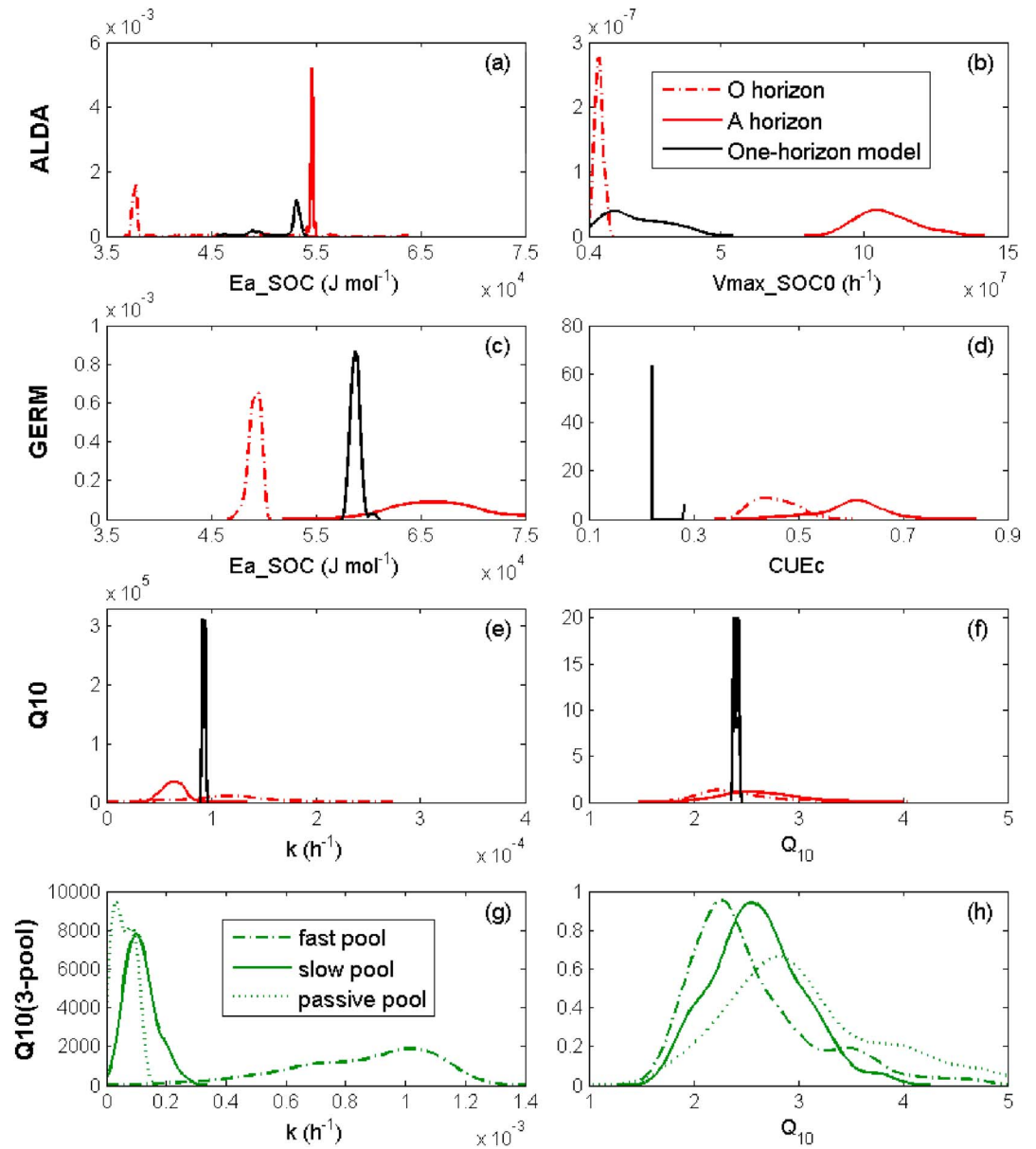[a]SD is the standard deviation of the corresponding metrics from ensemble optimization runs.
**Coefficient is significant at $p < 0.05$.

decomposability (Ea_SOC, activation energy; k) and microbial sensitivity to temperature (Q10, CUE) all exhibited a well-defined unimodal distribution but with different variation. The posterior PDF can also be a non-Gaussian distribution in a few cases (e.g., microbial turnover rate in two-horizon GERM model, optimum soil moisture content in two-horizon Q10 model, Figures S2 and S3 in the supporting information). In general, parameters for the A horizon were less constrained than those for the O horizon as the PDF was relatively flat with large standard deviations. This is likely because the field-based estimate of CO_2 flux is a convolution of both horizons, and the A horizon likely contributes less to the total flux because of its lower temperature and poorer substrate quality, thus lacking enough variation (information) to constrain the parameters for this horizon. Such unsymmetrical informativeness is a common challenge for data assimilation of multiple horizon decomposition models [*Keenan et al.*, 2012a; *Schädel et al.*, 2013]. Additional data streams such as incubation data or other pool-specific measurements may provide the necessary constraints to reduce posterior PDF uncertainty [*Keenan et al.*, 2012a]. The decomposition rate (k, Figure 3g) of fast SOC pool in the three-pool Q10 model was poorly constrained, probably because the small proportion of light fraction soil makes its CO_2 flux outweighed by that of the slow and passive pools (0.04–0.14 in Table 1 and 0.02–0.1 in posterior distribution of the corresponding parameter, see Figure S7 in the supporting information).

Ranges of parameter posterior PDF also reveal characteristics of SOC decomposition dynamics. The intrinsic decomposability of the A horizon is lower than that of the O horizon across all two-horizon models
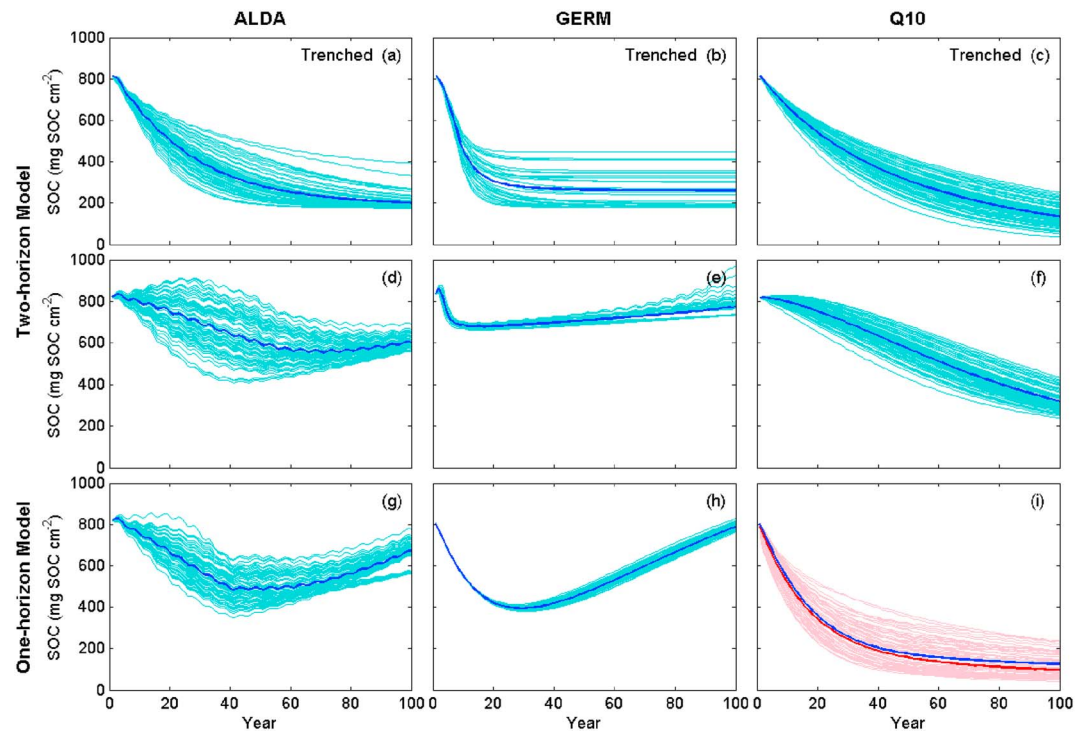

Figure 2. Observed and simulated soil efflux from the three soil decomposition models. (a–c) The two-horizon versions; (d–f) the one-horizon versions. The red lines in Figure 2f represent the results from the three-pool Q10 model. Error bar shows the uncertainty of simulated CO_2 efflux from 100 ensemble runs.

Figure 3. (a–f) Posterior parameter probability density function (PDFs) of three soil decomposition models. The O and A horizons represent the PDFs from the corresponding soil horizon from two-horizon models; one horizon represents the PDFs from the one-horizon models. (g and h) The results from the three-pool Q10 model. The range of the x axis indicates the range of the parameter's prior uniform distribution.

Table 3. Descriptions of a Subset of Model Parameters Mentioned in the Text

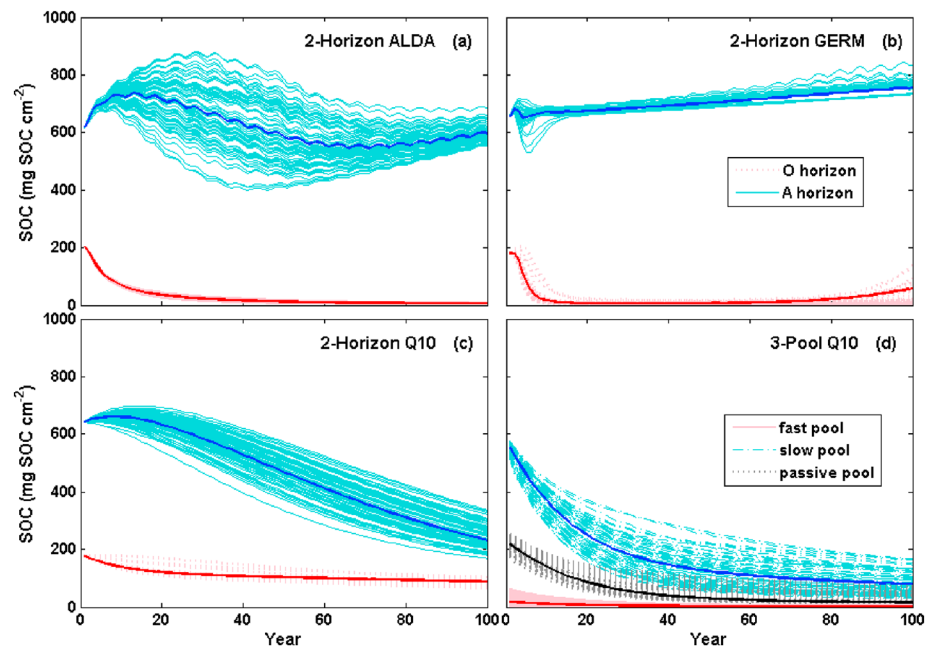| Parameter	Unit	Description
Ea_SOC	$J\,mol^{-1}$	Activation energy of decomposing SOC to soluble C
Vmax_SOC0	mg decomposed SOC cm^{-3} soil (mg ENZ cm^{-3} soil)$^{-1}$ h^{-1}	Maximum rate of converting SOC to soluble C
CUEc	%	Carbon use efficiency at temperature of 15°C
k	% h^{-1}	Intrinsic SOC decomposition rate
Q_{10}	-	Temperature sensitivity of decomposition rate to every 10°C change in temperature

Figure 4. Simulated 100 years responses of SOC stock for the three models. (a–c) Trenched plot simulation; (d–i) Model simulations under 4.8°C progressive increasing soil temperature and litterfall. The deep blue and red lines (for three-pool Q10 model) represent ensemble mean from the 100 independent optimization runs for each model, the light colored lines are the results from each ensemble member.

(Figures 3a, 3c, and 3e), indicating that C in deeper soils is more recalcitrant. Deeper soils also had higher Q10, suggesting higher temperature sensitivity of heterotrophic microorganisms at that depth (Figures 3d, 3f, and 3h), in line with field experiments from other studies [*Lefèvre et al.*, 2013; *Peng et al.*, 2009; *Zhou et al.*, 2009]. As expected, the one-horizon model parameters mostly fell within the mode of the analogous parameters for the O and A horizons in the two-horizon models, suggesting an averaging effect when lumping heterogeneous soil horizons together. Note that the CUE in the one-horizon GERM model is notably lower than that of two-horizon model, suggesting a nonlinear interaction structure among parameters (Figures S8–S10 in the supporting information).

3.2. Structural Difference Induced Discrepancy in Future SOC Stock Trajectory

The future projections of the trenched plot differed among the three two-horizon models (Figures 4a–4c). The initial ~5 years SOC stock was similar across all models, where models were constrained by observations and better model observation matches were achieved. However, the uncertainty in parameter posterior PDF caused diverging responses within each model. Intermodel variation was notable as SOC loss in both microbial models (ALDA and GERM) leveled off after 20 to 40 years, while the Q10 model was still losing C after 100 years. The difference among models was more notable in the litterfall + warming experiments. In the microbial models (ALDA and GERM), the enhanced respiration was compensated by increased litterfall input, so that at the end of 100 years, there was less than 250 mg SOC cm^{-2} difference from the initial SOC stock (Figures 4d and 4e). In contrast, the Q10 model was still losing SOC despite increased litterfall (Figure 4f). The overall trend in one-horizon models was similar to that of corresponding two-horizon models, except that both microbial models showed a greater SOC loss around 20 to 40 years (Figures 4g–4i), but this loss was later compensated by increasing litterfall similar to what occurred for the two-horizon models. The one-pool Q10 model and the ensemble mean of the three-pool Q10 model showed very similar SOC trajectories, although the one-pool Q10 model had much smaller uncertainty range (Figure 4i). Our results demonstrated two different types of uncertainty in decomposition models: (1) uncertainty associated with poorly constrained parameters (i.e., the multiple optima problem) [*Brun et al.*, 2001; *Duan et al.*, 1992] and (2)
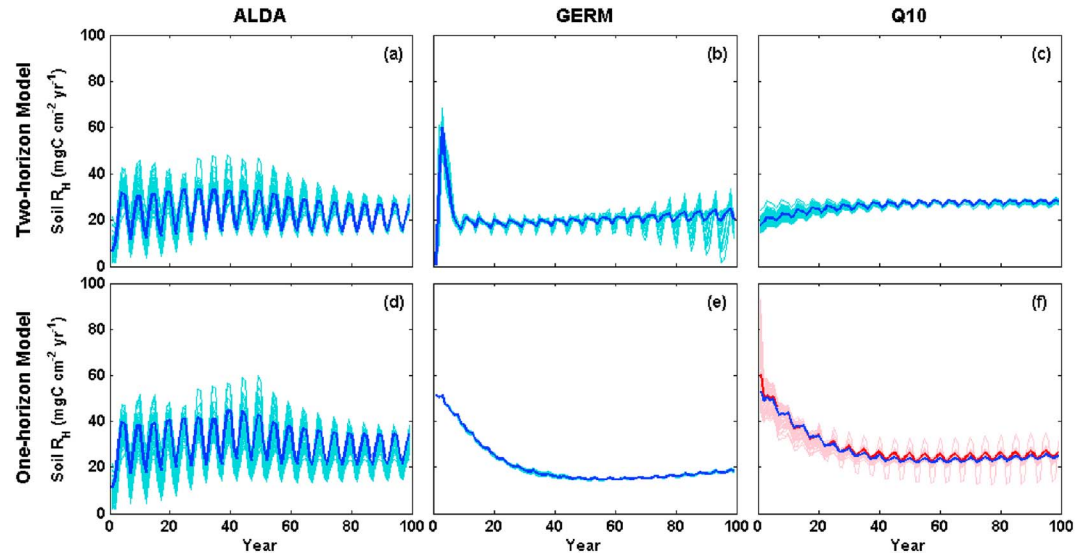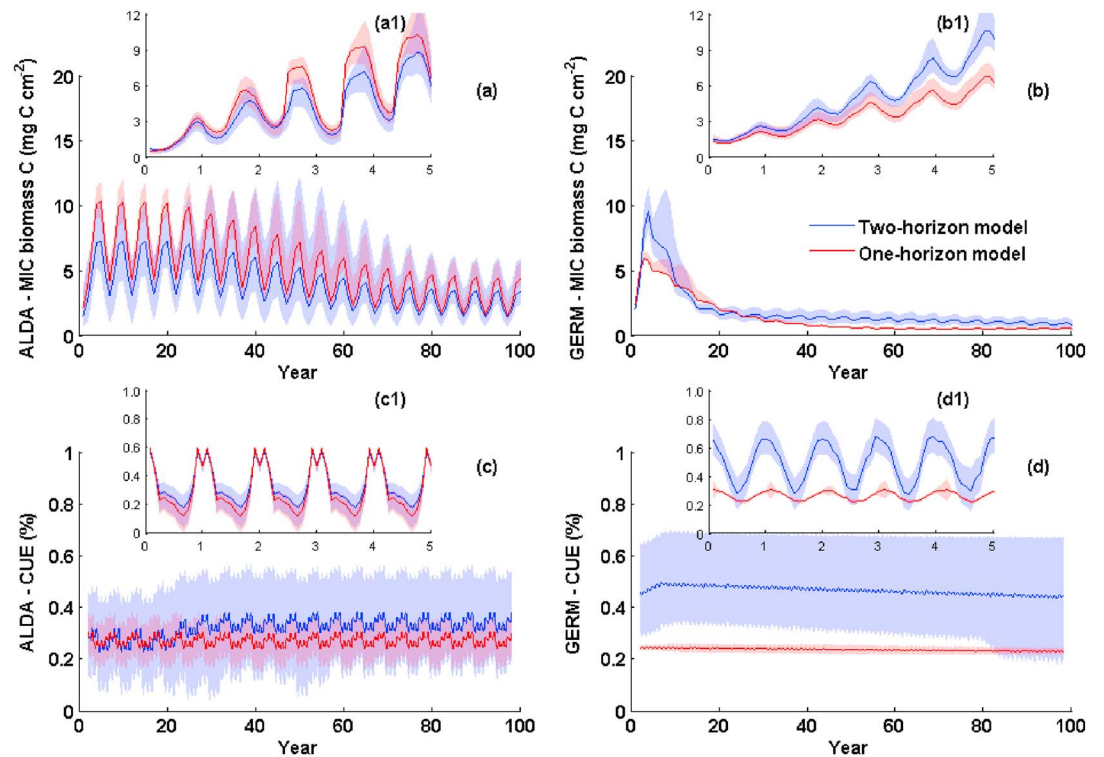
Figure 5. Simulated 100 years responses of SOC stock for each of the horizons for the two-horizon models and three-pool Q10 model. The deep blue and red lines (for three-pool Q10 model) represent ensemble mean from the 100 independent optimization runs for each model, the light colored lines are the results from each ensemble member.

the uncertainty associated with conceptual structure of the model (i.e., system identification), which fundamentally relies on our current scientific understanding of the system and its mathematical or numerical representation. While the first issue may be partially attributed to limitations inherent in the inverse estimation approach, the nonlinear structure of decomposition model (and any process-based biogeochemical model) also leads to the existence of multiple optima [*Duan et al.*, 1992]. Improved data assimilation techniques may help reduce parameter uncertainty in model calibration and projection [*Keenan et al.*, 2012b; *Koffi et al.*, 2012; *Parrish et al.*, 2012; *Zhou et al.*, 2013], but the uncertainty embedded in model structure (often due to imperfect understanding of the real system) is usually ignored and sometimes difficult to be disclosed by data assimilation alone, as shown in our results.

Detailed examination of various modeled processes help identify key features of different model structures. Both microbial models (ALDA and GERM), either one- or two-horizon models, had their labile horizon (O horizon) depleted within the first 20 years (Figures 5a and 5b) and the A horizon switched from losing C to eventually become a C sink. A similar labile C depletion was exhibited in the three-pool Q10 model, but not the two-horizon Q10 model (Figures 5c and 5d), likely because there was not enough information (e.g., an informative prior for decomposition rate) to differentiate the decomposition rate among the two horizons (PDF of decomposition rate of O horizon is quite flat, indicating high parameter uncertainty, Figure 3e). Projected soil R_H also diverged across models, with ALDA and two-horizon GERM models having exhibited a notable initially enhanced R_H upon warming for about 5 years and then stabilized at a similar level (Figures 6a, 6b, and 6d), although ALDA model has a much larger oscillation in soil R_H due to the same oscillation in microbial biomass (Figure 7a). Overall, for the depletion of labile C, warming enhanced R_H and loss of SOC which later attenuated and SOC loss eventually being compensated by increased litterfall of ALDA and GERM model matched the observed C dynamics in long-term soil warming experiments [*Kirschbaum*, 2004; *Knorr et al.*, 2005; *Luo et al.*, 2001; *Melillo et al.*, 2011]. Despite the oscillatory behavior of microbial models which may be improved by multipool representations (especially ALDA, see discussion of oscillation in section 3.3), their future projections matched better with observations than the conventional Q10 models, supporting our second hypothesis. Site level parameterization of microbial decomposition models probably require more measurements to be able to constrain parameters well (under-parameterized, tend to have high biases), while a simple Q10 type of model is likely to be overparameterized (high variance) with good calibration results but may fail when tested under different scenarios.

Figure 6. Simulated 100 years soil R_H for the three models. The deep blue and red lines (for three-pool Q10 model) represent ensemble mean from the 100 independent optimization runs for each model, the light colored lines are the results from each ensemble member.

Figure 7. (a, b, a1, and b1) Microbial biomass C and (c, d, c1, and d1) CUE changes in the ALDA and the GERM models (two-horizon and one-horizon models) under warming plus litterfall model simulations. Annual microbial biomass and 30 day moving average of hourly CUE are shown in Figures 7a–7d; seasonal microbial biomass and CUE dynamics for the first 5 years are shown in embedded graphs, Figures 7a1–7d1.

There are several limitations of this study that need to be explored further to make the results more generally applicable. First, our hierarchy of models was applied to a limited data set which is specific to a particular ecosystem and soil type. A more comprehensive study that covers various ecosystems and soil properties would help to separate ecosystem-specific recommendations for model selection from more generalized conclusions. Second, this limited data set also imposes a certain structure on our model in that the two-horizon model is composed of O and A horizons for the larch forest we tested. Models should be conceptually tailored to match the ecosystem characteristics being simulated. If the models were to be applied in a grassland ecosystem, which generally does not possess an O horizon, then a one-horizon model or a multilayer model with parameters that correspond to observed depth-resolved decomposition properties may be appropriate. Third, we assumed constant soil moisture for future scenarios and did not include a feedback of soil moisture to soil temperature. This feedback could result in a different SOC trajectory than what we presented, yet the divergent model response probably would still exist due to the model structures. Fourth, in our long-term extrapolation, an implicit assumption was that the model structure and represented processes are appropriate for the simulation period. Such an assumption is debatable. An option to address model structural uncertainty is Bayesian model averaging where a dynamic range of model structures are weighted by their posterior model probability [*Hoeting et al.*, 1999; *Wasserman*, 2000].

We also acknowledge that we are limited to only 4 years of observations to inform the model and that a longer period of observation (decadal to multidecadal) would have provided tighter constraints. This is especially true given the slow turnover rate of SOC. The importance and difficulty of constraining parameters associated with slow decomposition processes was also recognized in a 12 year study in a temperate deciduous forest in the Eastern U.S. [*Braswell et al.*, 2005]. For an efficient assimilation, data length is only one aspect, data quality and the amount of information encompassed by the observation are also critical [*Liu and Gupta*, 2007]. We argue that from the perspective of efficient data assimilation, other characteristics of the soil system (e.g., microbial-related features) can help identify proper parameters that will constrain the modeling system and thus should be included in the model. Note however that because the Q10 model has only one variable (i.e., SOC stock) that can be evaluated, the increased availability of other soil-related data (e.g., measured CUE, MIC pool sizes [*Frey et al.*, 2013; *Serna-Chavez et al.*, 2013]) cannot further inform the Q10 model. Without the support of sufficiently long and diverse observations to inform the model, model structure becomes a dominating factor in the future projection of SOC. It is worthy to note here that under the warming + litterfall scenario, the trajectories of the three models can differ notably from each other. Therefore, observations from warming manipulations or other manipulating experiments would be very valuable for informing models, as parameters should be better constrained.

3.3. Structural Difference Induced Discrepancy in Microbial Activity

In this study, different conceptual structures of microbial models led to different response trajectories. Annual average microbial biomass in both the ALDA and GERM models exhibited an initial increase and leveled off around year 60 and year 40, respectively (Figures 7a and 7b). Oscillatory behavior of microbial models has been analytically demonstrated by *Wang et al.* [2013] and is exhibited in the interannual variation of MIC of the two models in this study. The amplitude is much greater in the ALDA model, which is likely caused by the sensitivity of microbial biomass to soil moisture variation in the model (Pearson correlation between MIC and soil moisture is 0.6, $p < 0.05$), a sensitivity that does not occur in GERM model as soil moisture was not represented. In our field measurements, soil moisture increased in the second and third year and then slightly declined in subsequent years; such interannual cyclic moisture variation drove the MIC response so that MIC tightly tracked the moisture in the ALDA model. The increased MIC at the beginning of the simulation likely reflects the microbial responses to existing root exudates and sloughed-off cells that cannot be accounted for by correcting measured CO_2 efflux using root biomass. The high sensitivity of microbial activity to rhizodeposition (or so-called "rhizosphere priming effect" [*Kuzyakov*, 2002]) suggests that microbial models should account for the interaction between root and microbial activities. The seasonal patterns of MIC in both models were similar with both featuring lower MIC during the growing season and accumulating during the winter (Figures 7a1 and 7b1). This agreed well with the previously reported observed seasonal dynamics of soil microbial biomass C for the same site [*Liu and Wang*, 2010].

The dynamics of CUE were also different between the two models, despite the similar seasonal dynamics where lower CUE occurs during the growing season than during the nongrowing season. Because the GERM model used prescribed CUE as a linearly decreasing function of temperature, CUE decreased consistently due to progressive warming (Figure 7d). In contrast, in the modified ALDA model, CUE was simulated as a function of the ratio between respired CO_2 and assimilated SOC, which were both explicitly controlled by environmental conditions. Therefore, CUE of the ALDA model did not vary much with temperature (Figure 7c). Note that the upward shift in CUE in the ALDA model around year 20 is caused by a depletion of the O horizon due to fast substrate assimilation (Figure 5a), in line with *Knorr et al.* [2005] and *Kirschbaum* [2004], where their modeling approaches suggested "substrate depletion" as an explanation for apparent thermal acclimation in soil respiration under warming climate. Given the fairly good inverse estimation results against field-based estimates of both models, we conclude that both changing and constant CUEs are plausible with increasing temperature. Note that the average MIC declined in the ALDA two-horizon model under warming scenario (Figure 7a), yet CUE increased due to depletion of the O horizon. This is because the activation energy that controls SOC enzymatic decay of the A horizon is smaller than that of microbial respiration (Figure S2, Ea_SOC_A0 < Ea_Sx_A0) indicating smaller temperature sensitivity, therefore, the amount of Soluble C (substrate) consumed relative to microbial biomass declined with warming.

It is worth noting here that the oscillation amplitude of microbial biomass in the two-horizon ALDA model is notably smaller than that of the one-horizon model, which may be due to a more heterogeneous architecture of the soil C pools. The oscillations arise because of tight coupling between microbial and SOC pools, yet this behavior might weaken with greater pool heterogeneity in microbial models. In reality, there are many organisms consuming chemically heterogeneous substrates on varying timescales. Such heterogeneity could dampen the oscillations.

It should also be acknowledged that we tested a simplified modeling framework because the decomposition model was not coupled to other key element cycles. Soil C sequestration under ambient and rising atmospheric CO_2 can be constrained directly by nitrogen availability and indirectly by nutrients that support N_2 fixation [*Hobbie et al.*, 2002; *van Groenigen et al.*, 2006]. Kinetic and stoichiometric constrains on microbial physiology also pose key controls over SOC decomposition dynamics [*Allison*, 2005; *Sinsabaugh et al.*, 2013]. Incorporating those interactions into models could produce even more realistic future SOC dynamics than the models used in this study.

4. Conclusion

In this study, we calibrated three structurally different soil organic matter decomposition models (Q10 and two microbial models with different complexities) against in situ soil efflux observations, each with two-horizon and one-horizon versions. The calibration and validation results showed that all models can reasonably simulate 4 years of field-based estimates of R_H from a forest plot. However, there were differences among the models' projected decomposition dynamics under increased temperature and litterfall. Our study has three main conclusions. First, effective data assimilation requires sufficient data length and information content. For soils with long turnover time, long period of observations and multiple data streams (e.g., microbial biomass and enzyme characteristics) are needed to adequately constrain the models. Second, conceptual understanding of the ecological mechanisms represented in models dominates the trajectory of model projections among models that assimilate the same data to constrain parameters. While all the models in our study produced similar decomposition dynamics early in the projected simulations, the long-term projections varied substantially across all models. This indicates that there is substantial uncertainty associated with microbial processes among the models. Finally, labile C depletion was observed in both two-horizon microbial models. The substrate depletion shifted the carbon use efficiency in the ALDA model to result in an efficiency level and SOC trajectory similar to that of the GERM model in which carbon use efficiency was prescribed to decline with increasing temperature. This suggests that both constant and variable carbon use efficiency are plausible when modeling future decomposition dynamics and that short-term (e.g., a few years) observations are not sufficient to inform model parameters of the long-term responses of microbial thermal adaption.

References

Allison, S. D. (2005), Cheaters, diffusion and nutrients constrain decomposition by microbial enzymes in spatially structured environments, *Ecol. Lett.*, *8*(6), 626–635.

Allison, S. D., M. D. Wallenstein, and M. A. Bradford (2010), Soil-carbon response to warming dependent on microbial physiology, *Nat. Geosci.*, *3*(5), 336–340.

Arora, V. K., J. F. Scinocca, G. J. Boer, J. R. Christian, K. L. Denman, G. M. Flato, V. V. Kharin, W. G. Lee, and W. J. Merryfield (2011), Carbon emission limits required to satisfy future representative concentration pathways of greenhouse gases, *Geophys. Res. Lett.*, *38*, L05805, doi:10.1029/2010GL046270.

Arora, V. K., G. J. Boer, P. Friedlingstein, M. Eby, C. D. Jones, J. R. Christian, G. Bonan, L. Bopp, V. Brovkin, and P. Cadule (2013), Carbon-concentration and carbon-climate feedbacks in CMIP5 Earth system models, *J. Clim.*, *26*(15), 5289–5314.

Bond-Lamberty, B., D. Bronson, E. Bladyka, and S. T. Gower (2011), A comparison of trenched plot techniques for partitioning soil respiration, *Soil Biol. Biochem.*, *43*(10), 2108–2114.

Boone, R. D. (1994), Light-fraction soil organic matter: Origin and contribution to net nitrogen mineralization, *Soil Biol. Biochem.*, *26*(11), 1459–1468.

Braswell, B. H., W. J. Sacks, E. Linder, and D. S. Schimel (2005), Estimating diurnal to annual ecosystem parameters by synthesis of a carbon flux model with eddy covariance net ecosystem exchange observations, *Glob. Chang. Biol.*, *11*(2), 335–355.

Brun, R., P. Reichert, and H. R. Künsch (2001), Practical identifiability analysis of large environmental simulation models, *Water Resour. Res.*, *37*(4), 1015–1030, doi:10.1029/2000WR900350.

Coleman, K., and D. S. Jenkinson (1996), *RothC-26.3—A Model for the Turnover of Carbon in Soil*, Springer, IACR-Rothamsted, Harpenden, U. K.

Davidson, E. A., S. Samanta, S. S. Caramori, and K. Savage (2012), The Dual Arrhenius and Michaelis–Menten kinetics model for decomposition of soil organic matter at hourly to seasonal time scales, *Glob. Chang. Biol.*, *18*(1), 371–384.

Drake, J. E., A. C. Oishi, M. A. Giasson, R. Oren, K. H. Johnsen, and A. C. Finzi (2012), Trenching reduces soil heterotrophic activity in a loblolly pine (*Pinus taeda*) forest exposed to elevated atmospheric [CO2] and N fertilization, *Agr. Forest. Meteorol.*, *165*, 43–52.

Duan, Q., S. Sorooshian, and V. Gupta (1992), Effective and efficient global optimization for conceptual rainfall-runoff models, *Water Resour. Res.*, *28*(4), 1015–1031, doi:10.1029/91WR02985.

Duan, Q., S. Sorooshian, and V. K. Gupta (1994), Optimal use of the SCE-UA global optimization method for calibrating watershed models, *J. Hydrol.*, *158*(3–4), 265–284.

Fan H., Q. Cai, and H. Wang (2004), Condition of soil erosion in phaeozem region of northeast China, *Journal of Soil and Water Conservation*, *18*.

Fan, Z., J. C. Neff, J. W. Harden, and K. P. Wickland (2008), Boreal soil carbon dynamics under a changing climate: A model inversion approach, *J. Geophys. Res.*, *113*, G04016, doi:10.1029/2008JG000723.

Frey, S. D., J. Lee, J. M. Melillo, and J. Six (2013), The temperature response of soil microbial efficiency and its feedback to climate, *Nat. Clim. Change*, *3*(4), 395–398.

Friedlingstein, P., P. Cox, R. Betts, L. Bopp, W. Von Bloh, V. Brovkin, P. Cadule, S. Doney, M. Eby, and I. Fung (2006), Climate-carbon cycle feedback analysis: Results from the C4MIP model intercomparison, *J. Clim.*, *19*(14), 3337–3353.

Friend, A. D., W. Lucht, T. T. Rademacher, R. Keribin, R. Betts, P. Cadule, P. Ciais, D. B. Clark, R. Dankers, and P. D. Falloon (2014), Carbon residence time dominates uncertainty in terrestrial vegetation responses to future climate and atmospheric CO_2, *Proc. Natl. Acad. Sci.*, *111*(9), 3280–3285.

German, D. P., K. R. Marcelo, M. M. Stone, and S. D. Allison (2012), The Michaelis–Menten kinetics of soil extracellular enzymes in response to temperature: A cross-latitudinal study, *Glob. Chang. Biol.*, *18*(4), 1468–1479.

Graham, S. L., P. Millard, J. E. Hunt, G. N. Rogers, and D. Whitehead (2012), Roots affect the response of heterotrophic soil respiration to temperature in tussock grass microcosms, *Ann. Bot.*, *110*(2), 253–258.

Hanson, P. J., N. T. Edwards, C. T. Garten, and J. A. Andrews (2000), Separating root and soil microbial contributions to soil respiration: A review of methods and observations, *Biogeochemistry*, *48*(1), 115–146.

He, Y., Q. Zhuang, J. W. Harden, A. D. McGuire, Z. Fan, Y. Liu, and K. P. Wickland (2014), The implications of microbial and substrate limitation for the fates of carbon in different organic soil horizon types of boreal forest ecosystems: A mechanistically based model analysis, *Biogeosciences*, *11*, 4477–4491.

Hobbie, S. E., K. J. Nadelhoffer, and P. Hogberg (2002), A synthesis: The role of nutrients as constraints on carbon balances in boreal and arctic regions, *Plant and Soil*, *242*(1), 163–170.

Hoeting, J. A., D. Madigan, A. E. Raftery, and C. T. Volinsky (1999), Bayesian model averaging: A tutorial, *Statistical Science*, *14*(4), 382–401.

Ise, T., C. M. Litton, C. P. Giardina, and A. Ito (2010), Comparison of modeling approaches for carbon partitioning: Impact on estimates of global net primary production and equilibrium biomass of woody vegetation from MODIS GPP, *J. Geophys. Res.*, *115*, G04025, doi:10.1029/2010JG001326.

Jassal, R. S., and T. A. Black (2006), Estimating heterotrophic and autotrophic soil respiration using small-area trenched plot technique: Theory and practice, *Agr. Forest. Meteorol.*, *140*(1), 193–202.

Keenan, T. F., E. A. Davidson, J. W. Munger, and A. D. Richardson (2012a), Rate my data: Quantifying the value of ecological data for the development of models of the terrestrial carbon cycle, *Ecol. Appl.*, *23*(1), 273–286.

Keenan, T. F., E. Davidson, A. M. Moffat, W. Munger, and A. D. Richardson (2012b), Using model-data fusion to interpret past trends, and quantify uncertainties in future projections, of terrestrial ecosystem carbon cycling, *Glob. Chang. Biol.*, *18*(8), 2555–2569.

Kirschbaum, M. U. F. (2004), Soil respiration under prolonged soil warming: Are rate reductions caused by acclimation or substrate loss?, *Glob. Chang. Biol.*, *10*(11), 1870–1877.

Knorr, W., I. C. Prentice, J. I. House, and E. A. Holland (2005), Long-term sensitivity of soil carbon turnover to warming, *Nature*, *433*(7023), 298–301.

Koffi, E. N., P. J. Rayner, M. Scholze, and C. Beer (2012), Atmospheric constraints on gross primary productivity and net ecosystem productivity: Results from a carbon-cycle data assimilation system, *Global Biogeochem. Cycles*, *26*, GB1024, doi:10.1029/2010GB003900.

Kuzyakov, Y. (2002), Review: Factors affecting rhizosphere priming effects, *Journal of Plant Nutrition and Soil Science*, *165*(4), 382.

Landsberg, J. J., and S. T. Gower (1997), *Applications of Physiological Ecology to Forest Management*, Academic Press, San Diego, Calif.

Lavigne, M., R. Foster, and G. Goodine (2004), Seasonal and annual changes in soil respiration in relation to soil temperature, water potential and trenching, *Tree Physiol.*, *24*(4), 415–424.

Lawrence, C. R., J. C. Neff, and J. P. Schimel (2009), Does adding microbial mechanisms of decomposition improve soil organic matter models? A comparison of four models using data from a pulsed rewetting experiment, *Soil Biol. Biochem.*, *41*(9), 1923–1934.

Lefèvre, R., et al. (2013), Higher temperature sensitivity for stable than for labile soil organic carbon—Evidence from incubations of long-term bare fallow soils, *Glob. Chang. Biol.*, *20*(2), 633–640.

Li, J., G. Wang, S. Allison, M. Mayes, and Y. Luo (2014), Soil carbon sensitivity to temperature and carbon use efficiency compared across microbial-ecosystem models of varying complexity, *Biogeochemistry*, 1–18, doi:10.1007/s10533-013-9948-8.

Liu, S., and C. Wang (2010), Spatio-temporal patterns of soil microbial biomass carbon and nitrogen in five temperate forest ecosystems, *Acta Ecologica Sinica*, *30*(12), 3135–3143.

Liu, Y., and H. V. Gupta (2007), Uncertainty in hydrologic modeling: Toward an integrated data assimilation framework, *Water Resour. Res.*, *43*, W07401, doi:10.1029/2006WR005756.

Lloyd, J., and J. Taylor (1994), On the temperature dependence of soil respiration, *Funct. Ecol.*, *8*(3), 315–323.

Luo, Y., S. Wan, D. Hui, and L. L. Wallace (2001), Acclimatization of soil respiration to warming in a tall grass prairie, *Nature*, *413*(6856), 622–625.

Mahecha, M. D., M. Reichstein, N. Carvalhais, G. Lasslop, H. Lange, S. I. Seneviratne, R. Vargas, C. Ammann, M. A. Arain, and A. Cescatti (2010), Global convergence in the temperature sensitivity of respiration at ecosystem level, *Science*, *329*(5993), 838–840.

Manzoni, S., P. Taylor, A. Richter, A. Porporato, and G. I. Ågren (2012), Environmental and stoichiometric controls on microbial carbon-use efficiency in soils, *New Phytol.*, *196*(1), 79–91.

Melillo, J. M., P. A. Steudler, J. D. Aber, K. Newkirk, H. Lux, F. P. Bowles, C. Catricala, A. Magill, T. Ahrens, and S. Morrisseau (2002), Soil warming and carbon-cycle feedbacks to the climate system, *Science*, *298*(5601), 2173–2176.

Melillo, J. M., et al. (2011), Soil warming, carbon–nitrogen interactions, and forest carbon budgets, *Proc. Natl. Acad. Sci.*, *108*(23), 9508–9512.

Oechel, W. C., G. L. Vourlitis, S. J. Hastings, R. C. Zulueta, L. Hinzman, and D. Kane (2000), Acclimation of ecosystem CO_2 exchange in the Alaskan Arctic in response to decadal climate warming, *Nature*, *406*(6799), 978–981.

Parrish, M. A., H. Moradkhani, and C. M. DeChant (2012), Toward reduction of model uncertainty: Integration of Bayesian model averaging and data assimilation, *Water Resour. Res.*, *48*, W03519, doi:10.1029/2011WR011116.

Parton, W. J., et al. (1993), Observations and modeling of biomass and soil organic matter dynamics for the grassland biome worldwide, *Global Biogeochem. Cycles*, *7*(4), 785–809, doi:10.1029/93GB02042.

Peng, S., S. Piao, T. Wang, J. Sun, and Z. Shen (2009), Temperature sensitivity of soil respiration in different ecosystems in China, *Soil Biol. Biochem.*, *41*(5), 1008–1014.

Schädel, C., E. A. G. Schuur, R. Bracho, B. Elberling, C. Knoblauch, H. Lee, Y. Luo, G. R. Shaver, and M. R. Turetsky (2013), Circumpolar assessment of permafrost C quality and its vulnerability over time using long-term incubation data, *Glob. Chang. Biol.*, *20*(2), 641–652.

Schädel, C., E. A. G. Schuur, R. Bracho, B. Elberling, C. Knoblauch, H. Lee, Y. Luo, G. R. Shaver, and M. R. Turetsky (2014), Circumpolar assessment of permafrost C quality and its vulnerability over time using long-term incubation data, *Glob. Chang. Biol.*, *20*(2), 641–652.

Schimel, D. S. (1995), Terrestrial ecosystems and the carbon cycle, *Glob. Chang. Biol.*, *1*(1), 77–91.

Schlesinger, W. H., and J. A. Andrews (2000), Soil respiration and the global carbon cycle, *Biogeochemistry*, *48*(1), 7–20.

Serna-Chavez, H. M., N. Fierer, and P. M. van Bodegom (2013), Global drivers and patterns of microbial abundance in soil, *Glob. Ecol. Biogeogr.*, *22*(10), 1162–1172.

Seth, A., S. A. Rauscher, M. Biasutti, A. Giannini, S. J. Camargo, and M. Rojas (2013), CMIP5 projected changes in the annual cycle of precipitation in monsoon regions, *J. Clim.*, *26*(19), 7328–7351.

Sierra, C. A. (2012), Temperature sensitivity of organic matter decomposition in the Arrhenius equation: Some theoretical considerations, *Biogeochemistry*, *108*(1), 1–15.

Silver, W. L., and R. K. Miya (2001), Global patterns in root decomposition: Comparisons of climate and litter quality effects, *Oecologia*, *129*, 407–419.

Sinsabaugh, R. L., S. Manzoni, D. L. Moorhead, and A. Richter (2013), Carbon use efficiency of microbial communities: Stoichiometry, methodology and modelling, *Ecol. Lett.*, *16*(7), 930–939.

Smith, N. G., and J. S. Dukes (2013), Plant respiration and photosynthesis in global-scale models: Incorporating acclimation to temperature and CO_2, *Glob. Chang. Biol.*, *19*(1), 45–63.

Tan, Z., R. Lal, L. Owens, and R. C. Izaurralde (2007), Distribution of light and heavy fractions of soil organic carbon as related to land use and tillage practice, *Soil Tillage Res.*, *92*(1–2), 53–59.

Todd-Brown, K. E. O., J. T. Randerson, W. M. Post, F. M. Hoffman, C. Tarnocai, E. A. G. Schuur, and S. D. Allison (2013), Causes of variation in soil carbon simulations from CMIP5 Earth system models and comparison with observations, *Biogeosciences*, *10*(3), 1717–1736.

Trumbore, S. E. (1993), Comparison of carbon dynamics in tropical and temperate soils using radiocarbon measurements, *Global Biogeochem. Cycles*, *7*(2), 275–290, doi:10.1029/93GB00468.

Tuomi, M., P. Vanhala, K. Karhu, H. Fritze, and J. Liski (2008), Heterotrophic soil respiration—Comparison of different models describing its temperature dependence, *Ecol. Model.*, *211*(1), 182–190.

van Groenigen, K.-J., J. Six, B. A. Hungate, M.-A. de Graaff, N. van Breemen, and C. van Kessel (2006), Element interactions limit soil carbon storage, *Proc. Natl. Acad. Sci.*, *103*(17), 6571–6574.

van't Hoff, J. H. (1898), *Lectures on Theoretical and Physical Chemistry, Part I. Chemical Dynamics* [translated by R. A. Lehfeldt], pp. 224–229, Edward Arnold, London.

Wang, C., and J. Yang (2007), Rhizospheric and heterotrophic components of soil respiration in six Chinese temperate forests, *Glob. Chang. Biol.*, *13*(1), 123–131.

Wang, C., J. Yang, and Q. Zhang (2006), Soil respiration in six temperate forests in China, *Glob. Chang. Biol.*, *12*(11), 2103–2114.

Wang, Y., B. Chen, W. Wieder, Y. Luo, M. Leite, B. Medlyn, M. Rasmussen, M. Smith, F. Agusto, and F. Hoffman (2013), Oscillatory behavior of two nonlinear microbial models of soil carbon decomposition, *Biogeosci. Discuss.*, *10*(12), 19,661–19,700.

Wasserman, L. (2000), Bayesian model selection and model averaging, *J. Math. Psychology*, *44*(1), 92–107.

Wickland, K. P., and J. C. Neff (2008), Decomposition of soil organic matter from boreal black spruce forest: Environmental and chemical controls, *Biogeochemistry*, *87*(1), 29–47.

Wieder, W. R., G. B. Bonan, and S. D. Allison (2013), Global soil carbon projections are improved by modelling microbial processes, *Nat. Clim. Change*, *3,* 909–912.

Yang, J., and C. Wang (2005), Soil carbon storage and flux of temperate forest ecosystems in northeastern China, *Acta Ecologica Sinica*, *25*(11), 2875–2882.

Yi, S., A. D. McGuire, E. Kasischke, J. Harden, K. Manies, M. Mack, and M. Turetsky (2010), A dynamic organic soil biogeochemical model for simulating the effects of wildfire on soil environmental conditions and carbon dynamics of black spruce forests, *J. Geophys. Res.*, *115*, G04015, doi:10.1029/2010JG001302.

Zhang, X., X. Wang, B. Zhu, Z. Zong, C. Peng, and J. Fang (2008), Litterfall production in relation to environmental factors in northeast China's forests [Chinese version with English abstract], *J. Plant Ecol.*, *32*(5), 1031–1040.

Zhao, S. (2013), *A Preliminary Study on the Characteristics of Temperature Forest Soil Organic Carbon*, 39 pp, Northeast Forestry Univ., Harbin, China.

Zhou, T., P. Shi, D. Hui, and Y. Luo (2009), Global pattern of temperature sensitivity of soil heterotrophic respiration (Q10) and its implications for carbon-climate feedback, *J. Geophys. Res.*, *114*, G02016, doi:10.1029/2008JG000850.

Zhou, T., P. Shi, G. Jia, and Y. Luo (2013), Nonsteady state carbon sequestration in forest ecosystems of China estimated by data assimilation, *J. Geophys. Res., Biogeosciences*, *118*, 1369–1384, doi:10.1002/jgrg.20114.